Structural and magnetic properties of stage-2 $EuCl_3$-graphite intercalation compound

Itsuko S. Suzuki, Masatsugu Suzuki, and Charles R. Burr
Department of Physics and Materials Research Center, State University of New York at Binghamton, Binghamton, New York 13902

D. M. Hwang
Bellcore, Red Bank, New Jersey 07701

Eberhard Stumpp
Department of Inorganic Chemistry, Technical University of Clausthal, 3392 Clausthal, Zellerfeld, Germany
(Received 6 August 1990)

Structural and magnetic properties of stage-2 $EuCl_3$-graphite intercalation compounds have been studied by using x-ray diffraction, electron diffraction, and dc magnetic susceptibility. The repeat distance along the c axis is 13.28 ± 0.02 Å. The $EuCl_3$ intercalate layer forms a three-layer sandwich of Cl-Eu-Cl, where the distance between Eu and Cl layers is 1.67 Å. The layer structure of the $EuCl_3$ intercalate layer is similar to that of YCl_3 type. The $EuCl_3$ layer is hexagonal with two Eu ions per unit cell (lattice constant 7.38 Å) and consists of domain structures generated by the rotation of the (3×3) commensurate structure with respect to the graphite lattice by $\pm6.3°$, $\pm10°$, $\pm13.8°$, and $\pm17.5°$. The $EuCl_3$ layer is modulated by the graphite layer. The dc magnetic susceptibility is found to be a sum of contributions from Eu^{2+} and Eu^{3+} ions. The concentrations of Eu^{3+} and Eu^{2+} in the $EuCl_3$ intercalate layer are 0.994 and 0.006, respectively. The susceptibility contribution from Eu^{2+} ions obeys the Curie-Weiss law with a Curie-Weiss temperature $\Theta=10.1\pm1.1$ K. The susceptibility contribution from the van Vleck ion Eu^{3+} is almost independent of temperature, where the energy difference between $^7F_0$ and $^7F_1$ levels is given by $E_1=538$ K.

I. INTRODUCTION

Magnetic graphite intercalation compounds (GIC's) provide an excellent opportunity for the study on the relationship between dimensionality and magnetism. In these compounds, the magnetic intercalate layers are periodically separated by a number (the stage number) of graphite layers in stacks along the c axis. The interplanar interaction between adjacent magnetic intercalate layers can be systematically reduced by increasing the stage number, while the intraplanar interaction remains virtually unchanged. Most of the relevant studies until now have dealt with transition-metal dichloride GIC's such as $CoCl_2$, $NiCl_2$, and $MnCl_2$ GIC.[1,2] In contrast to these compounds, there have been few systematic studies on physical properties of rare-earth metal trichloride GIC's as far as we know. Stumpp[3] has reported his success in synthesizing GIC's with all lanthanide trichlorides from $SmCl_3$ to $LuCl_3$ as intercalants. The pristine $SmCl_3$ and $EuCl_3$ have a structure of UCl_3 type with three-dimensional (3D) bonding, while the pristine $DyCl_3$, $HoCl_3$, $ErCl_3$, $TmCl_3$, $YbCl_3$, and $LuCl_3$ have a structure of YCl_3 type with two-dimensional (2D) bonding.[4,5] Note that the pristine $EuCl_3$ is hexagonal with two Eu ions per unit cell (space group $P6_3/m$).[6,7] The unit cell parameters are $a=7.3746$ Å and $c=4.1323$ Å.[5] The Eu ions are located on symmetry sites at $\pm(\frac{1}{3},\frac{2}{3},\frac{1}{4})$ and the chloride ions on mirrors at $\pm(x,y,\frac{1}{4};\ -y,x-y,\frac{1}{4};\ y-x,-x,\frac{1}{4})$ with $x=0.389\,11$ and $y=0.301\,74$. The pristine YCl_3 is monoclinic with two Y ions per unit cell (space group $C2/m$).[8] The lattice parameters are $a=6.92$ Å, $b=11.94$ Å, $c=6.44$ Å, and $\beta=111.0°$. The Y ions are located in octahedral holes between alternate pairs of close-packed layers of Cl ions. For the $DyCl_3$, $HoCl_3$, $ErCl_3$, $TmCl_3$, $YbCl_3$, and $LuCl_3$ GIC's, the structure of intercalate layers may be similar to that of the pristine trichlorides because of 2D bonding. For the $SmCl_3$ and $EuCl_3$ GIC's, it is expected that the structure of the intercalate layers may change from UCl_3 type with 3D bonding to YCl_3 type with 2D bonding.

With considerable progress in sample preparation,[3,9] rare-earth metal trichloride GIC's have become available for the study of structural and magnetic properties. Until now we know of measurements of ^{151}Eu Mössbauer and optical reflectivity only for a mixed stage-2 and -3 $EuCl_3$ GIC sample based on highly oriented pyrolytic graphite (HOPG).[10] Recently we have succeeded in synthesizing a well-defined stage-2 $EuCl_3$ GIC sample based on single-crystal Kish graphite (SCKG). In this paper we report first the structural and magnetic properties of the stage-2 $EuCl_3$ GIC which are obtained from the measurements of x-ray scattering, electron diffraction, and dc magnetic susceptibility. We investigate (i) the in-plane structure of the $EuCl_3$ intercalate layer, (ii) the layer structure of the $EuCl_3$ intercalate layer (YCl_3 or UCl_3 type), (iii) the staging structure along the c axis, and (iv) the magnetic properties including the magnetic phase transition.

II. EXPERIMENT

A powdered $EuCl_3$ sample was freshly prepared by heating a mixture of $EuCl_3 \cdot 6H_2O$ and NH_4Cl in a HCl stream at 500 °C. A mixture of $EuCl_3$ and SCKG was sealed in a quartz tube with Cl_2 gas at 1 atm, and kept at 600 °C for 5 weeks. The GIC sample thus obtained was thoroughly washed with dimethylformamide to remove excess $EuCl_3$, which remained unreacted on the surface of samples. The c-axis stacking sequence of this compound was confirmed by (00L) x-ray diffraction to be well-defined stage-2.

The dc magnetic susceptibility measurements of this compound were made with a Cahn electrobalance with an applied magnetic field H oriented perpendicular to the c axis of the crystal. The GIC sample of 37.27 mg was placed in a fused quartz sample holder of known susceptibility. The dc magnetic susceptibility was measured from 35 to 300 K at 4.0 kOe and from 1.3 to 35 K at 100 Oe. The (00L) x-ray diffraction to this compound was performed by using a Huber double-circle diffractometer (1.5 kW) with Mo $K\alpha$ radiation source to determine the structure of the intercalate layer. Electron diffraction was also carried out to determine the in-plane structure of the $EuCl_3$ intercalate layer using a JEOL 4000FX transmission electron microscope operated at 400 keV. The electron diffraction pattern was obtained from several parts of a sample with a selected area diffraction aperture of 0.27 μm.

III. RESULT AND DISCUSSION

A. Structural properties

We have carried out (00L) x-ray diffraction experiments on the stage-2 $EuCl_3$ GIC sample at 300 K. Figure 1 shows the (00L) x-ray diffraction pattern where the wave number along the c^* direction is given by $Q_c = L(2\pi/d)$ and the c-axis repeat distance is $d = 13.28 \pm 0.02$ Å. It is found that rather sharp Bragg reflections are observed at $L = 1, 2, \ldots, 16$. The full width at half maximum (FWHM) ΔQ seems to be independent of the index L for $2 \le L \le 8$: $\Delta Q = 0.050$ Å^{-1} at $L = 3$, and 0.048 Å^{-1} at $L = 8$. This result indicates that there is little Hendricks-Teller-type staging disorder in this sample. Usually, a "well-defined" stage-2 sample may still have small fractions of packages with stages 1 and 3. For a stage-2 $CoCl_2$ GIC sample based on SCKG, for example, the random arrangement of packages with different stages along the c axis gives rise to the oscillatory behavior of FWHM of Bragg reflections with the index L, which has a minimum at $L = 4$ and maximum at $L = 6$.[11]

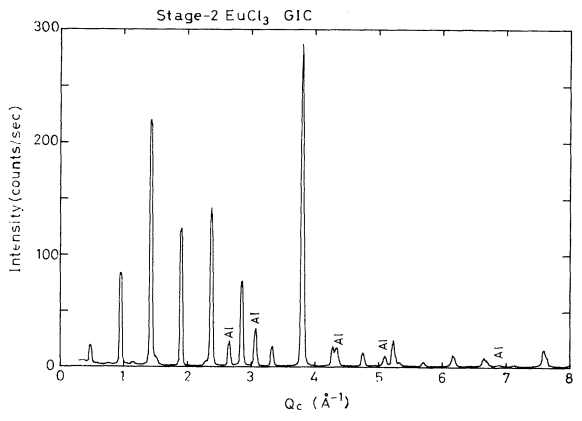

FIG. 1. (00L) x-ray diffraction pattern for the stage-2 $EuCl_3$ GIC at 300 K, where $Q_c = L(2\pi/d)$ with c-axis repeat distance $d = 13.28$ Å. The Bragg peaks from the Al sample holder are denoted by Al.

To examine the structure of the $EuCl_3$ intercalate layer in the stage-2 $EuCl_3$ GIC from the intensity analysis of (00L) Bragg reflections, we consider the following three models for the structure of the $EuCl_3$ intercalate layer. (i) The $EuCl_3$ intercalate layer consists of a three-layer sandwich of Cl-Eu-Cl, where the distance between the Eu layer and the Cl layer is given by $z(\neq 0)$. (ii) The intercalate layer consists of two layers. Both Eu and Cl ions are located on each layer, where the distance between the two layers is given by $2z_1$. If $EuCl_3$ is intercalated into the graphite host without change of structure, the intercalate layer is assumed to have this type of layer structure. (iii) The intercalate layer consists of a single layer on which both Eu and Cl ions are located. This model corresponds to model (i) with $z = 0$, or model (ii) with $z_1 = 0$.

For models (i) and (iii), a package of C-Cl-Eu-Cl-C-C is assumed to align periodically along the c axis. The distance between C-Cl-Eu-Cl-C is $2c_1 = 9.93$ Å and the distance between C-C is 3.35 Å. Then the x-ray scattering intensity along the Q_c [$= L(2\pi/d)$] direction is expressed by

$$I(00Q_c) = A|S(Q_c)|^2 e^{-B(Q_c/4\pi)^2} , \tag{1}$$

with

$$|S(Q_c)|^2 = [2\rho_G f_G(Q_c)\cos(Q_c c_1) + 2\rho_{Cl} f_{Cl}(Q_c)\cos(Q_c z) + \rho_{Eu} f_{Eu}(Q_c)]^2 . \tag{2}$$

Here A is a constant, the exponential factor with a constant B is a Debye-Waller factor used by Baron *et al.*[12] to calculate the (00L) x-ray intensity of $MnCl_2$ GIC. f_G, f_{Cl}, and f_{Eu} are the atomic form factors of C, Cl, and Eu atoms, and ρ_G, ρ_{Cl}, and ρ_{Eu} are the number of C, Cl, and Eu atoms per unit area and are described by

$$\rho_G = \frac{n}{2}, \quad \rho_{Cl} = \frac{3+\delta}{2}, \quad \rho_{Eu} = 1 , \tag{3}$$

for the stage-2 $EuCl_3$ GIC with stoichiometry of $C_n EuCl_{3+\delta}$. The weight uptake measurement of the sample for the x-ray scattering experiment before and after intercalation leads to the relation $n = 17.8 + 2.44\delta$, where δ is the number of extra chlorine atoms. The least-squares fit of the integrated intensity of Bragg reflections with $L = 1-16$ in Fig. 1, to Eq. (1) yields the values of $A = 0.755$, $z = 1.67$ Å, $\delta = 0.2$, and $B = 7.4$. The value of δ is in good agreement with that determined from chemi-

cal analysis by Boolchand *et al.*[10] The agreement between observed and calculated intensities is very good, as listed in Table I.

For model (ii), the x-ray scattering intensity along the Q_c [$=L(2\pi/d)$] direction is expressed by Eq. (1) with

$$|S(Q_c)|^2=\{2\rho_G f_G(Q_c)\cos(Q_c c_1) +2[\rho_{Cl}f_{Cl}(Q_c)+\rho_{Eu}f_{Eu}(Q_c)] \times\cos(Q_c z_1)\}^2 , \quad (4)$$

and

$$\rho_G=\frac{n}{2},\ \rho_{Cl}=\frac{3+\delta}{2},\ \rho_{Eu}=\tfrac{1}{2} . \quad (5)$$

The agreement between the integrated x-ray intensity and calculated intensity is poor for any permitted values of A, z_1, δ, and B, indicating that model (ii) is not suitable for explaining our experimental results of (00L) x-ray scattering. Then we can conclude that the structure of the intercalate layer can be well described by model (i). The $EuCl_3$ intercalate layer consists of a three-layer sandwich of Cl-Eu-Cl, where the distance between Eu and Cl layers is $z=1.67$ Å. This layer structure is similar to that of YCl_3 type. The stage-2 $EuCl_3$ GIC sample used in the present work has a stoichiometry $C_{18.3}EuCl_{3.2}$, indicating an excess of 0.2 above that associated with EuCl3.

It is well accepted for transition metal chloride GIC's such as $CoCl_2$, $MnCl_2$, $NiCl_2$, and $FeCl_3$ GIC that (i) the intercalate layer is formed of small islands and (ii) the excess chlorine atoms on the periphery of the islands may provide acceptor sites to charges transferred from the graphite layer. Here we assume that this mechanism of charge transfer also works for the stage-2 $EuCl_3$ GIC. For the $EuCl_3$ intercalate layer having the stoichiometry of $EuCl_{3+\delta}$, the fractional chlorine excess f is defined by $f=\delta/3$. According to Wertheim,[13] the value of f is given, in terms of the island radius R, as the ratio of the number of Eu atoms on the boundary of the island to three times the number of Eu atoms inside the island, yielding

$$f=\frac{p\left[\frac{2\pi\sqrt{3}R}{b}\right]}{3\left[\frac{4\pi R^2}{\sqrt{3}b^2}\right]}=p\left[\frac{b}{2R}\right] , \quad (6)$$

where p is a geometrical factor and is on the order of unity, but is a little larger than unity. This expression is somewhat different from that derived by Wertheim [$f=b/(2\sqrt{3}R)$].[13] The value of f is estimated as 0.2/3 since the stoichiometry of our sample is given by $C_{18.3}EuCl_{3.2}$. As will be shown later, the in-plane lattice constant is determined as $b=3\times2.46$ Å$=7.38$ Å from the electron diffraction pattern. From Eq. (6) the island size can be calculated as $2R=pb/f=111p$ Å. The island size is on the order of 100–200 Å if $p\approx1$–2.

We have performed electron diffraction experiments on the stage-2 $EuCl_3$ GIC at 300 K to determine the in-plane structure of the $EuCl_3$ intercalate layer. Figure 2(a) shows a typical in-plane diffraction pattern of the stage-2 $EuCl_3$ GIC sample, which was used for the (00L) x-ray diffraction of Fig. 1. The Bragg reflections from the graphite and $EuCl_3$ layers are denoted by large and small circles, respectively. This pattern shows an eightfold splitting in each Bragg reflection of $EuCl_3$ layers. Note that we also observed an in-plane diffraction pattern having no splitting of Bragg reflections for a very thin area of the same sample, indicating the existence of a single domain.

Here we present a model for the in-plane structure of the $EuCl_3$ intercalate layer that explains the complicated diffraction pattern of Fig. 2(a). In our model, the $EuCl_3$ intercalate layer is hexagonal with two Eu ions per unit cell as the pristine $EuCl_3$. The unit cell dimension b ($=7.38$ Å) is three times larger than that of the graphite lattice ($=2.46$ Å), forming the (3×3) commensurate structure. This lattice constant b is almost the same as that of the pristine $EuCl_3$ ($=7.3746$ Å). The eightfold splitting of the Bragg reflections from $EuCl_3$ layers indicates that the $EuCl_3$ intercalate layer consists of eight domains in which the (3×3) commensurate structure is rotated by $\theta=\pm6.3°$, $\pm10°$, $\pm13.8°$, and $\pm17.5°$ with respect to the graphite layer, respectively.

Figure 2(b) shows the schematic ($HK0$) reciprocal lattice plane, which is derived from our model. Bragg reflections from the graphite layer and the $EuCl_3$ layers are located at wave vectors $\mathbf{Q}=\{\mathbf{G}_i\}$ and $\{\mathbf{K}_i\}$, respectively, where $\mathbf{G}_i$ and $\mathbf{K}_i$ are the fundamental reciprocal lattice vectors of graphite and $EuCl_3$ layers with $|\mathbf{G}_i|=2.95$ Å^{-1}, $|\mathbf{K}_i|=|\mathbf{G}_i|/3=0.983$ Å^{-1}, $\mathbf{G}_1+\mathbf{G}_2$

TABLE I. Experimental integrated intensity and calculated intensities of Bragg reflections in the (00L) x-ray scattering for stage-2 $EuCl_3$ GIC. The calculated intensities are given by Eq. (1) with $A=0.755$, $B=7.4$, $d=13.28$ Å, $z_1=1.67$ Å, and $\delta=0.2$.

L	I_{expt}	I_{calc}
1	763	452
2	1898	2455
3	5678	5413
4	3015	3005
5	2994	3070
6	1604	1507
7	372	485
8	5908	5921
9	378	388
10	273	360
11	496	467
12	100	75
13	225	205
14	180	142
15	35	49
16	333	331

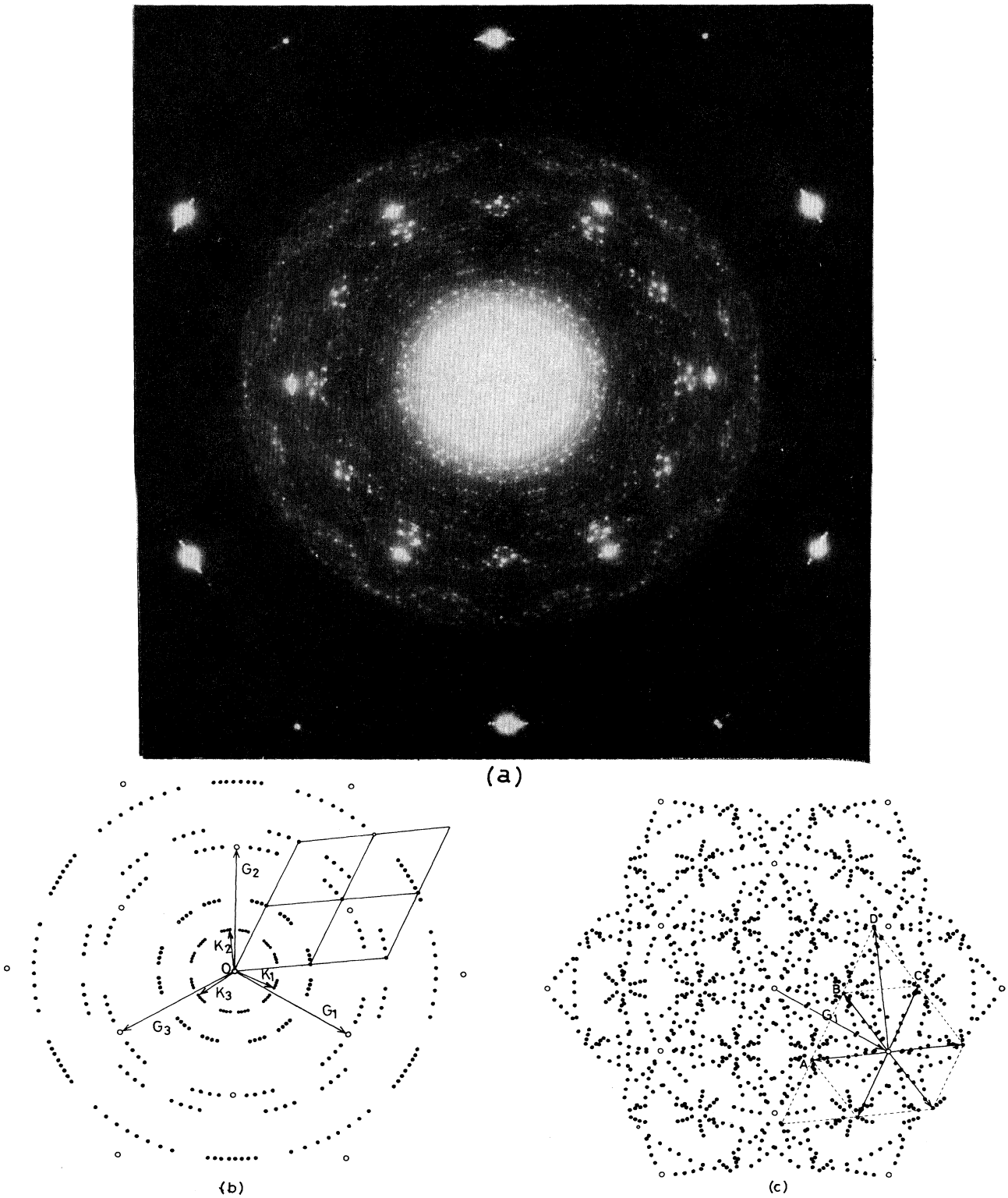

FIG. 2. (a) In-plane electron diffraction pattern of stage-2 $EuCl_3$ GIC at 300 K. (b) Schematic ($HK0$) reciprocal lattice plane for stage-2 $EuCl_3$ GIC. Bragg reflections from the graphite and $EuCl_3$ layers are denoted by open and closed circles, respectively. The wave vectors $\mathbf{G}_i$ and $\mathbf{K}_i$ are the fundamental reciprocal lattice vectors of graphite and $EuCl_3$ layers with $|\mathbf{G}_i|=2.95$ Å^{-1} and $|\mathbf{K}_i|=|\mathbf{G}_i|/3=0.983$ Å^{-1}. The eightfold splitting is due to the eight equivalent orientations of the commensurate (3×3) structure with respect to the graphite layer. One of the eight equivalent orientations is shown. (c) Schematic interpretation of (a), where the Bragg reflections are located at $\{\mathbf{G}\pm\mathbf{K}\}$ where $\{\mathbf{G}\}$ and $\{\mathbf{K}\}$ are the sets of the reciprocal lattice vectors of graphite and $EuCl_3$ layers, respectively.

$+\mathbf{G}_3=0$, and $\mathbf{K}_1+\mathbf{K}_2+\mathbf{K}_3=0$. The wave vectors $\{\mathbf{G}_i\}$ and $\{\mathbf{K}_i\}$ are the sets of reciprocal lattice vectors of graphite and $EuCl_3$ layers, respectively, and are described by $\{\mathbf{G}_i\}=h\mathbf{G}_1+k\mathbf{G}_2$ (h and k are integers) and $\{\mathbf{K}_i\}=p\mathbf{K}_1+q\mathbf{K}_2$ (p and q are integers). In Fig. 2(b), $\{\mathbf{K}_i\}$ is the reciprocal lattice vector of the $EuCl_3$ layer which is obtained by the rotation of the (3×3) commensurate structure by $\theta=+6.3°$ with respect to the graphite lattice. The angle between vectors $\mathbf{G}_1$ and $\mathbf{K}_1$ is $\theta=+6.3°$. This is one of the eight equivalent patterns, and coincides with the in-plane diffraction pattern observed by us for the single domain sample. The extinction rule for the 2D hexagonal lattice with two Eu ions shows that the intensity of Bragg reflections at $\mathbf{Q}=\{\mathbf{K}_i\}$ with $p+q=3m$ (m is an integer) is much stronger than that of Bragg reflections with $p+q\neq3m$ for $L=0$. At the present we do not know about the stacking sequence of the $EuCl_3$ layers along the c axis in this compound. If this compound has a stacking sequence of α-β-γ type, the intensity of Bragg reflections with $p+q\neq3m$ is reduced to zero at $L=0$. For simplicity, only the Bragg reflections with $p+q=3m$ are shown in Fig. 2(b).

The complicated electron diffraction pattern of Fig. 2(a) is explained by assuming that the $EuCl_3$ intercalate layer is modulated by the graphite potential. The 2D hexagonal Eu lattices are subjected to lateral periodic potentials due to the rigid graphite lattice. The static distortion from the ideal hexagonal lattice position ($\mathbf{R}_i$) of Eu ions, $\mathbf{v}(\mathbf{R}_i,\mathbf{R}_0)$, can be described by

$$\mathbf{v}(\mathbf{R}_i,\mathbf{R}_0)=\sum_{\mathbf{G}}\mathbf{u}_{\mathbf{G}}\sin[\mathbf{G}\cdot(\mathbf{R}_i-\mathbf{R}_0)]\ , \tag{7}$$

where $\mathbf{R}_0$ is the origin of potential of graphite and $|\mathbf{u}_{\mathbf{G}}|$ is much smaller than the lattice constant. Then the scattering intensity $I(\mathbf{Q})$ is given by[14]

$$I(\mathbf{Q})=E\left[\sum_{\mathbf{K}}\delta(\mathbf{Q}-\{\mathbf{K}\})+\sum_{\mathbf{G},\mathbf{K}}|\mathbf{u}_{\mathbf{G}}\cdot\mathbf{Q}|^2\delta(\mathbf{Q}-\{\mathbf{G}\pm\mathbf{K}\})\right], \tag{8}$$

where $\{\mathbf{G}\pm\mathbf{K}\}$ is a combination of $\{\mathbf{G}_i\}$ and $\{\mathbf{K}_i\}$, and E is a constant. The first term of Eq. (8) yields the Bragg reflections at $\mathbf{Q}=\{\mathbf{K}\}$ from the ideal hexagonal lattice. The second term is due to the periodic modulation with wave vector $\mathbf{G}$, and gives rise to the sidebands at $\mathbf{Q}=\{\mathbf{G}\pm\mathbf{K}\}$. Figure 2(c) shows the position of these sidebands on the $(HK0)$ reciprocal lattice plane. Each graphite reflection is surrounded by the Bragg reflections from the $EuCl_3$ layer. The sidebands around the graphite reflection ($\mathbf{G}_1$) are shown in Fig. 2(c). These sidebands are located at $\mathbf{Q}=\mathbf{G}_1-2\mathbf{K}_1-\mathbf{K}_2$ (point A), $\mathbf{G}_1-\mathbf{K}_1+\mathbf{K}_2$ (point B), $\mathbf{G}_1+\mathbf{K}_1+2\mathbf{K}_2$ (point C), $\mathbf{G}_1+3\mathbf{K}_2$ (point D), and so on. The in-plane diffraction pattern of Fig. 2(a) seems to agree qualitatively with the schematic $(HK0)$ reciprocal lattice plane of Fig. 2(c). The intensity of the sidebands is proportional to $|\mathbf{u}_{\mathbf{G}}\cdot\mathbf{Q}|^2$, which is characteristic of the static distortion of the $EuCl_3$ layer by the graphite potential. In Fig. 2(a), the intensity of Bragg reflections A and B of the sidebands around the graphite reflection $\mathbf{G}_1$ seems to be stronger than the Bragg reflections at $\{\mathbf{K}_i\}$. This suggests that the distortion $|\mathbf{u}_{\mathbf{G}}|$ from the uniform hexagonal lattice may be fairly large. Thus we can conclude that (i) the $EuCl_3$ layer is hexagonal; (ii) the $EuCl_3$ intercalate layer consists of eight domains in which the (3×3) commensurate structures are rotated by $\theta=\pm6.3°$, $\pm10°$, $\pm13.8°$, and $\pm17.5°$ with respect to the graphite layer; and (iii) the $EuCl_3$ layer is modulated by the graphite potential.

B. Magnetic properties

Figure 3 shows the dc magnetic susceptibility of the stage-2 $EuCl_3$ GIC perpendicular to the c axis, as a function of temperature. No magnetic phase transition is observed at temperatures above 1.5 K. In order to analyze these data, we assume that Eu sites in the $EuCl_3$ intercalate layer are occupied by Eu^{2+} ions and Eu^{3+} ions in the concentration ratio of c: $(1-c)$ with $0\leq c\leq1$. The ground state of the Eu^{2+} ion is ${}^8S_{7/2}$ with $(4f)^7$ electron configuration, so that each Eu^{2+} ion has spin $S=\frac{7}{2}$ with zero orbital angular momentum. The ground state of Eu^{3+} is a nondegenerate ${}^7F_0$. There exist J-state levels of ${}^7F_1$, ${}^7F_2$, and ${}^7F_3$ states above the ground state ${}^7F_0$. For the pristine $EuCl_3$, the energy difference between ground state and these three levels are 355.05 cm^{-1} (=510.84 K), 1022.54 cm^{-1} (=1471.2 K), and 1846.77 cm^{-1} (=2657.10 K).[15] Then the dc magnetic susceptibility $\chi(T)$ is assumed to be a sum of susceptibility contribu-

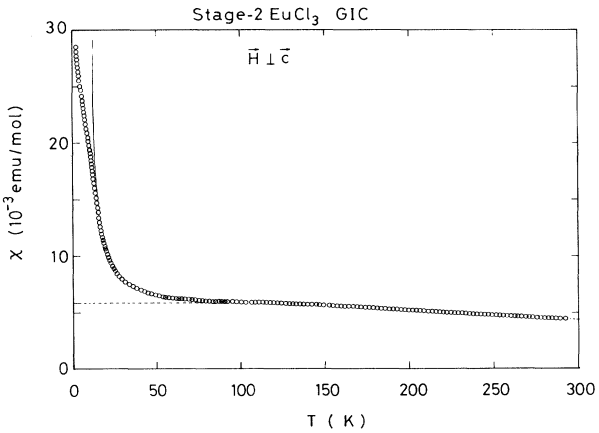

FIG. 3. dc magnetic susceptibility of stage-2 $EuCl_3$ GIC perpendicular to the c axis as a function of temperature. The theoretical susceptibility, given Eq. (9) with all parameters shown in the text, is denoted by the solid line. The theoretical susceptibility from the Eu^{3+} and core diamagnetism is denoted by dotted line.

tions from Eu^{2+} and Eu^{3+},

$$\chi(T)=c\chi_{Eu^{2+}}(T)+(1-c)\chi_{Eu^{3+}}(T)+\chi_{core} . \quad (9)$$

Here the susceptibility from Eu^{2+} obeys the Curie-Weiss law and is given by[16]

$$\chi_{Eu^{2+}}=\frac{C_M}{T-\Theta} , \quad (10)$$

with the Curie-Weiss constant C_M and Curie-Weiss temperature Θ. The theoretical value of C_M for Eu^{2+} is given by $C_M=(N_A\mu_B^2/3k_B)[g\sqrt{\mathbf{J}(\mathbf{J}+1)}]^2=7.8745$ emu K/Eu mol where g is a Landé factor ($g=2$) and $\mathbf{J}=\frac{7}{2}$. For the donor type GIC, stage-1 Eu GIC (C_6Eu), Eu ion is found to exist as Eu^{2+}. The dc magnetic susceptibility of C_6Eu for the direction perpendicular to the c axis obeys the Curie-Weiss law with $C_M=6.78$ emu K/Eu mol, and $\Theta=1.3\pm1.0$ K.[17] Since Eu^{3+} is a van Vleck ion, the susceptibility from Eu^{3+} is given by[16]

$$\chi_{Eu^{3+}}=\frac{N_A\mu_B^2}{k_B}\left\{\left[\frac{8}{E_1}+\left[\frac{4.5}{T}+\frac{15}{E_2-E_1}-\frac{8}{E_1}\right]e^{-E_1/T}\right]\Big/(1+3e^{-E_1/T})\right\} . \quad (11)$$

Here E_1 and E_2 are the energy differences between $^7F_0$ and $^7F_1$, and between $^7F_0$ and $^7F_2$, respectively. When $E_1=511$ K and $E_2=1471$ K are used to calculate the temperature dependence of Eu^{3+} susceptibility, it is found that the Eu^{3+} susceptibility is almost independent of temperature below 50 K, and is assumed to be equal to the value at $T=0$ K, which is theoretically given by $\chi_{Eu^{3+}}(0)=(N_A\mu_B^2/k_B)(8/E_1)$. In Eq. (9), χ_{core} is the diamagnetic core susceptibility, which is independent of temperature and is estimated as $\chi_{core}=-213\times10^{-6}$ emu/Eu mol for the stoichiometry of $C_{18.3}EuCl_{3.2}$ by using the following diamagnetic core susceptibility values: -6×10^{-6} emu/mol for C, -26×10^{-6} emu/mol for Cl^-, -20×10^{-6} emu/mol for Eu^{3+}, and -22×10^{-6} emu/mol for Eu^{2+}.[18] Since the diamagnetic core susceptibility of Eu^{2+} is almost the same as that of Eu^{3+}, the diamagnetic core susceptibility is assumed to be independent of concentration c. Note that here the value for Eu^{3+} is adopted as the value for Eu in the calculation of χ_{core}. Then dc magnetic susceptibility of the stage-2 $EuCl_3$ GIC can be simply expressed by

$$\chi(T)=\frac{cC_M}{T-\Theta}+\chi_0 , \quad (12)$$

below 50 K, where χ_0 is the temperature-independent susceptibility and is described by

$$\chi_0=(1-c)\chi_{Eu^{3+}}(0)+\chi_{core} . \quad (13)$$

The least-squares fit of the dc magnetic susceptibility data, taken in the temperature range between 20 and 50 K, to Eq. (12) yields the values of $cC_M=4.9\times10^{-2}$ (emu K/Eu mol), $\Theta=10.1\pm1.1$ K, and $\chi_0=5.33\times10^{-3}$ emu/Eu mol. If the theoretical value of C_M for Eu^{2+} ($=7.8745$ emu K/Eu mol) is used, the concentration of Eu^{2+} is estimated as $c=0.006$. If the value of C_M ($=6.78$ emu K/Eu mol) determined for Eu^{2+} in C_6Eu is used, then the value of c is determined as $c=0.007$. This result implies that 99.4% of Eu sites in the $EuCl_3$ intercalate layer are occupied by Eu^{3+}, which is slightly different from the result derived by Boolchand *et al.*[10] They have found from ^{151}Eu Mössbauer experiments on the mixed stage-2 and -3 $EuCl_3$ GIC based on HOPG that Eu is present only as Eu^{3+} in the $EuCl_3$ intercalate layer. We believe that the dc susceptibility at low temperature is much more sensitive to the concentration of Eu^{2+} compared to the ^{151}Eu Mössbauer experiment, because the dc susceptibility from Eu^{2+} is much larger than that from Eu^{3+} at low temperatures.

The positive value of Θ indicates that the intraplanar exchange interaction J between Eu^{2+} ions is ferromagnetic. The Curie-Weiss temperature Θ is expressed in terms of J as

$$\Theta=\frac{2Z}{3}[(g-1)^2\mathbf{J}(\mathbf{J}+1)]J . \quad (14)$$

Here note that the component of spin $\mathbf{S}$ along the $\mathbf{J}$ direction is given by $(g-1)\mathbf{J}$. Since $\mathbf{J}=S=\frac{7}{2}$, and $g=2$ for Eu^{2+}, the expression for the Curie-Weiss temperature Θ reduces to the conventional form in terms of spin S,

$$\Theta=\frac{2ZJ}{3}S(S+1) , \quad (15)$$

where Z is the number of nearest-neighbor Eu atoms in the intercalate layer ($Z=3$). From Eq. (15) the value of J is determined as $J=0.32$ K. The susceptibility from Eu^{3+} at 0 K is obtained by subtracting χ_{core} from χ_0: $\chi_{Eu^{3+}}(0)=5.54\times10^{-3}/(1-c)=5.58\times10^{-3}$ emu/Eu mol with $c=0.006$. The energy difference E_1 between $^7F_0$ and $^7F_1$ can be calculated from the value of $\chi_{Eu^{3+}}(0)$ as $E_1=538$ K, which is a little larger than the value of E_1 reported for the pristine $EuCl_3$. In Fig. 3 also shown is the theoretical susceptibility using Eq. (9) with all parameters determined by our analysis. The agreement between experiment and theory is excellent except for low temperatures below 20 K, verifying the simple model that the susceptibility of Eu^{2+} and Eu^{3+} is additive. The deviation of the experimental data from the theoretical susceptibility Eq. (9) below 20 K may be due to a short-range spin order which may begin to grow around 20 K

through the ferromagnetic intraplanar exchange interaction J (=0.32 K), although no magnetic phase transition of this compound is observed above 1.5 K.

IV. CONCLUSION

We have investigated the structural and magnetic properties of the stage-2 $EuCl_3$ GIC with a stoichiometry of $C_{18.3}EuCl_{3.2}$ by x-ray, electron diffraction, and dc magnetic susceptibility measurements. The $EuCl_3$ intercalate layer consists of a three-layer sandwich of Cl-Eu-Cl where the separation between Eu layer and Cl layer is $z=1.67$ Å. The repeat distance along the c axis is 13.28 ± 0.02 Å. This indicates that the layer structure of the $EuCl_3$ intercalate layers changes from UCl_3 type with 3D bonding to that of YCl_3 type with 2D bonding. The $EuCl_3$ layer is hexagonal with two Eu ions per unit cell (lattice constant 7.38 Å), and consists of eight domain structures in which the (3×3) commensurate structure is rotated by $\pm6.3°$, $\pm10°$, $\pm13.8°$, and $\pm17.5°$ with respect to the graphite lattice. The $EuCl_3$ intercalate layer is formed of small islands, which diameter is on the order of 100–200 Å. The excess chlorine of 0.2 existing in the form of $EuCl_{3.2}$ may exist on the periphery of these islands and provide acceptor sites for charge transfer from the graphite layer. It has been revealed through the dc magnetic susceptibility that 0.6% and 99.4% of Eu sites are occupied by Eu^{2+} and Eu^{3+} ions. The existence of Eu^{2+} is confirmed from the susceptibility contribution from Eu^{2+}, showing a Curie-Weiss law with $\Theta=10.1$ K below 50 K. The susceptibility contribution from Eu^{3+} ion shows a van Vleck susceptibility with $E_1=538$ K, which is almost independent of temperature. No magnetic phase transition is observed at temperatures above 1.5 K from the dc magnetic susceptibility. We plan to do the ac susceptibility of this compound in the future to examine the possibility of magnetic phase transition.

ACKNOWLEDGMENTS

The authors would like to thank W. Brinkman and L. F. Tien for their help on the dc magnetic susceptibility measurement. They are grateful to H. Suematsu and Y. Hishiyama for providing good quality of single crystal Kish graphites. The work at the State University of New York at Binghamton (M.S.) was supported by the National Science Foundation, Grant No. DMR-8902351.

[1]G. Dresselhaus, J. T. Nicholls, and M. S. Dresselhaus, in *Graphite Intercalation Compounds II,* edited by H. Zabel and S. A. Solin (Springer-Verlag, Berlin, 1990).
[2]M. Suzuki, CRC Crit. Rev. Solid State Mater. Sci. **16**, 237 (1990).
[3]E. Stumpp. Mater. Sci. Eng. **31**, 53 (1977).
[4]A. F. Wells, *Structural Inorganic Chemistry,* 3rd ed. (Oxford University Press, New York, 1962).
[5]*Structural Chemistry of Layer-Type Phases,* edited by F. Levy (Reidel, Dordrecht, 1976).
[6]D. H. Templeton and C. H. Dauben, J. Am. Chem. Soc. **76**, 5237 (1954).
[7]B. Morosin, J. Chem. Phys. **49**, 3007 (1968).
[8]D. H. Templeton and G. F. Carter, J. Phys. Chem. **58**, 940 (1954).
[9]E. Stumpp and G. Nietfeld, Z. Anorg. Allg. Chem. **456**, 261 (1979).
[10]P. Boolchand, G. Lemon, W. J. Bresser, D. H. McDaniel, P. C. Eklund, R. E. Heinz, E. Stumpp, and G. Nietfeld, Solid State Commun. **52**, 675 (1984).
[11]I. S. Suzuki, M. Suzuki, L. F. Tien, and C. R. Burr, Phys. Rev. B (to be published).
[12]F. Baron, S. Flandrois, C. Hauw, and J. Gaultier, Solid State Commun. **42**, 759 (1982).
[13]G. K. Wertheim, Solid State Commun. **38**, 633 (1981).
[14]M. Suzuki, H. Ikeda, H. Suematsu, Y. Endoh, and M. T. Hutchings, J. Phys. Soc. Jpn. **49**, 671 (1980).
[15]J. A. Sommers and E. F. Westrum, Jr., J. Chem. Thermodyn. **9**, 1 (1977).
[16]P. Wachter, in *Valence Instabilities and Related Narrow-Band Phenomena,* edited by R. D. Parks (Plenum, New York, 1977), p. 337.
[17]H. Suematsu, K. Ohmatsu, and R. Yoshizaki, Solid State Commun. **38**, 1103 (1981).
[18]L. N. Mulay, *Magnetic Susceptibility* (Interscience, New York, 1966).

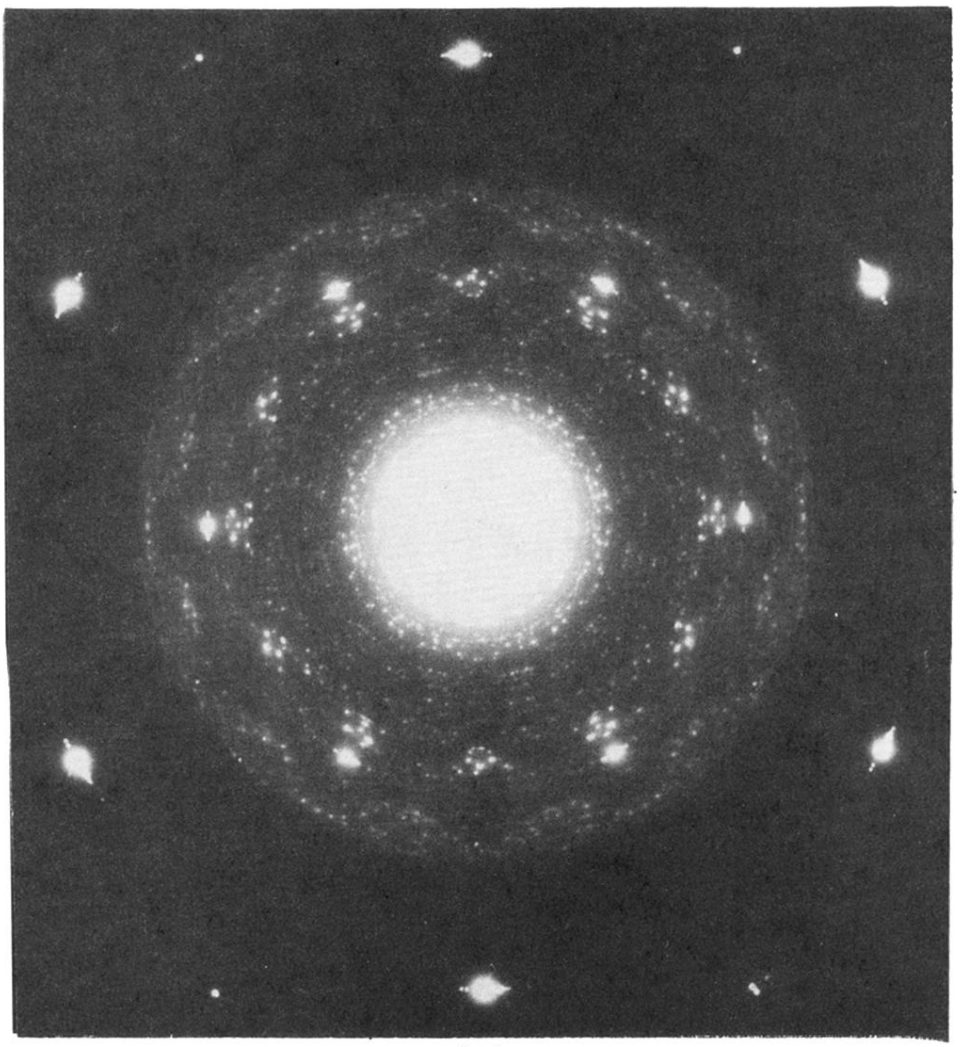

FIG. 2. (a) In-plane electron diffraction pattern of stage-2 $EuCl_3$ GIC at 300 K. (b) Schematic ($HK0$) reciprocal lattice plane for stage-2 $EuCl_3$ GIC. Bragg reflections from the graphite and $EuCl_3$ layers are denoted by open and closed circles, respectively. The wave vectors $\mathbf{G}_i$ and $\mathbf{K}_i$ are the fundamental reciprocal lattice vectors of graphite and $EuCl_3$ layers with $|\mathbf{G}_i|=2.95$ Å^{-1} and $|\mathbf{K}_i|=|\mathbf{G}_i|/3=0.983$ Å^{-1}. The eightfold splitting is due to the eight equivalent orientations of the commensurate (3×3) structure with respect to the graphite layer. One of the eight equivalent orientations is shown. (c) Schematic interpretation of (a), where the Bragg reflections are located at $\{\mathbf{G}\pm\mathbf{K}\}$ where $\{\mathbf{G}\}$ and $\{\mathbf{K}\}$ are the sets of the reciprocal lattice vectors of graphite and $EuCl_3$ layers, respectively.